International Journal of Pharmaceutics 400 (2010) 176–182

Contents lists available at ScienceDirect

International Journal of Pharmaceutics

journal homepage: www.elsevier.com/locate/ijpharm

Pharmaceutical Nanotechnology

The role of vehicle–nanoparticle interactions in topical drug delivery

Mojgan Moddaresi[a,c], Marc B. Brown[b], Yanjun Zhao[a,d], Slobodanka Tamburic[c], Stuart A. Jones[a,*]

[a] Pharmaceutical Science Division, King's College, London 150 Stamford St, London, SE1 9NH, United Kingdom
[b] School of Pharmacy, University of Hertfordshire, College Lane, Hatfield, AL10 9AB, United Kingdom
[c] School of Science and Management, London College of Fashion, 20 John Prince's Street, London, W1G OBJ, United Kingdom
[d] School of Pharmaceutical Science & Technology, Tianjin University, 92 Weijin Road, Tianjin, 300072, China

ARTICLE INFO

Article history:
Received 15 December 2009
Received in revised form 5 August 2010
Accepted 10 August 2010
Available online 18 August 2010

Keywords:
Lipid nanoparticles
Rheology
Permeation
Topical formulation
Nanoparticle tracking

ABSTRACT

Loading 'difficult to deliver' therapeutic agents into lipid nanoparticles (LN) is an attractive means to administer them to the skin. However, employing colloidal carriers to administer therapeutic agents from semi-solid preparations adds an extra dimension to the already complex process of topical drug delivery. The aim of this work was to understand how the mobility of nanoparticles influenced the delivery of a model drug when the carriers were suspended in a hyaluronic acid (HA) vehicle. Tocopheryl acetate (TA) was loaded into lipid nanoparticles (TA_{LN}) that were <100 nm in size and physically stable for more than 28 days. The TA_{LN} interacted with the HA polymeric chains to increase formulation macroviscosity. Nanoparticle tracking analysis confirmed that the gel hindered the TA_{LN} mobility. However, deliberate manipulation of the particle mobility in the gel by varying the concentration of HA had little effect on TA delivery. Only ca. 10 $\mu g/cm^2$ of administered TA was delivered into porcine skin regardless of the vehicle characteristics and this suggested that drug release from the LN was the rate limiting step in the delivery process and not the nanoparticle–vehicle–skin interactions.

1. Introduction

There have been several reports that loading therapeutic agents into nanoparticles can enhance drug delivery into skin (Kreuter et al., 1983; Scherer, 1992; Santos Maia et al., 2000). However, in most cases, compared to when a drug is solubilised in a topical vehicle, the drug delivery rate is reduced when a particulate carrier is employed. This is because enclosing a therapeutic agent within a particle adds a second rate limiting step that retards the drug presentation to its intended site of delivery (Muller and Kreuter, 1999; Ricci et al., 2005). As a consequence of their greater complexity and slower drug release, particulate systems are usually only employed for topical delivery when attempting to deliver 'difficult to formulate' agents. Such compounds require the delivery system to be carefully designed in order to resolve a particular problem. In this context nanocarriers have been shown to be particularly effective at promoting: skin occlusion (Jenning et al., 1999); chemical protection (Dingler et al., 1998); controlled release (Jenning et al., 2000a); colour/odour masking and drug loading in topical vehicles (Dingler et al., 1996).

It is now widely accepted that nanoparticles with a size of greater than 10 nm do not penetrate the skin to any great extent (Baroli et al., 2007; Ryman-Rasmussen et al., 2006). However, the question of whether particle–skin interactions influence drug release from nanocarriers has yet to be answered. Very little is known about the rate of particle diffusion in topical formulations. As a consequence it is unclear if altering the diffusion of particles in semi-solid vehicles influences drug delivery. A good understanding of the nanoparticle–vehicle–skin interaction is important as it will dictate the size of the nanoparticles and the properties of the vehicles that should be used in topical preparations to achieve the desired release profile. For example, smaller particles may release a drug more rapidly due to a higher surface area, but if held immobile in a gel they may never reach the skin surface. As it is not known if the presentation of a particle at the lipid skin surface encourages drug release, it is unclear if viscous vehicles pose a problem to effective delivery of drugs from semi-solid preparations containing nanocarriers (Jenning et al., 2000b).

Nanoparticle mobility in simple matrices has been assessed by spectroscopic techniques but such methods have not been applied to topical gels (Spiedel et al., 2003). The current knowledge of particle mobility through gels is derived from traditional diffusion cell experiments. For example, Sanders et al. (2000), used sputum from cystic fibrosis patients to show that nanoparticle diffusion was extremely slow (<0.5% of particles diffused through the barrier). Nanoparticle diffusion in mucus demonstrates a strong dependence on particle size with the smallest sized particles being retarded the least by the complex crosslinked gel network of this viscous excretion. The gel network of semi-solid drug delivery vehicles is more homogeneous than respiratory mucus, but the rate of nanoparticle

* Corresponding author.
E-mail address: stuart.jones@kcl.ac.uk (S.A. Jones).

0378-5173/$ – see front matter © 2010 Elsevier B.V. All rights reserved.
doi:10.1016/j.ijpharm.2010.08.012

permeation will be dependent upon similar properties such as the gel viscosity, type and extent of cross linking and polymeric chain chemistry of the semi-solid vehicles.

Loading poorly water soluble compounds in an aqueous topical gel can be facilitated by encapsulation within nanoparticles. A nanocarrier system is preferable to an ointment, which would traditionally be employed to solubilise a hydrophobic agent, in terms of cosmetic acceptability. Previous work has shown that nanoparticles can alter the viscosity of a gel as a consequence of the particles facilitating association of the macromolecular chains in the matrix (Chi and Jun, 1991; Rafiee-Tehrani and Mehramizi, 2000). How such changes in the gel macroviscosity influence drug delivery has not been elucidated. Therefore, the aim of this study was to characterise the interactions of loaded lipid nanoparticle with a hydrophilic gel suitable for topical drug delivery. In order to achieve this aim, TA was chosen as a model lipophilic active; the active was loaded into lipid nanoparticles (LN) and formed into a homogeneous HA gel. HA–nanoparticle interactions were characterised by traditional 'cone and plate' rheometry, while nanoparticle tracking analysis (NTA) measured the nanoparticle mobility in the gel. TA delivery from two gels that restricted the freedom of the drug loaded nanoparticles to very different degrees was assessed using porcine skin as a model.

2. Materials

A mixture of medium chain acid triglycerides (Labrafac® WL 1349) was provided by Gattefossé S.A. (France). Soybean lecithin (Lipoid® S75-3) was donated by Lipoid Gmbh (Germany), a mixture of free polyethylene glycol 660 and polyethylene glycol 660 hydroxystearate (Solutol® HS 15) were provided by BASF (Univar, UK) and D-α tocopheryl acetate (96.0–102.0% purity) by Roche (Adina chemicals, UK). Sodium chloride, ethanol and methanol (high performance liquid chromatography, HPLC grade) were purchased from VWR (UK). Sodium hyaluronate powder (HA) (average molecular weight of 550,000 Da), and caprylic-capric acid triglycerides (Miglyol 810) were generous gifts from MedPharm (UK) and SBlack (UK), respectively.

3. Methods

3.1. Nanoparticle production and loading

Both placebo (P_{LN}) and TA loaded LN (TA_{LN}) were prepared by a phase-inversion process described previously by Heurtault et al. (2002). Briefly, TA oil (4%, w/w, if required) was dissolved in a Labrafac (16.5%, w/w), Lipoid S-75 (1.75%, w/w) and Solutol (16.25%, w/w) mixture that was dispersed in an aqueous phase (NaCl in water, at 61.5%, w/w). The dispersion was heated and stirred to just above the phase inversion temperature (PIT) of the system (ca. 90 °C). The emulsion was homogenised by repeating this heating process between 55 °C and 90 °C at a rate of approximately 4 °C/min, 3 times. The LN were generated from the o/w emulsion by adding cool water (0 °C) to the mixture at the end of the last of the three heating cycles. The TA_{LN} were purified by ultracentrifugation (L7 ultracentrifuge, Beckman, USA) at 40,000 rpm for 1 h using temperature of 20 °C to generate $TA_{LN\text{-}PURE}$. Three layers were produced and the nanoparticles extracted from the middle layer of the three. The purified solution was used for all the topical formulations. TA content of the particles was determined using a HPLC assay and the TA loading and the total TA recovery were calculated (Eqs. (1) and (2)):

$$\text{TA loading}\,(\%) = \frac{\text{C2}\,(\text{mg})}{\text{C1}\,(\text{mg})} \times 100 \quad (1)$$

$$\text{TA recovery}\,(\%) = \frac{\text{Ctotal}\,(\text{mg})}{\text{C1}\,(\text{mg})} \times 100 \quad (2)$$

where C1 was the initial amount of TA added, C2 was the amount of TA recovered from the nanoparticles and Ctotal was total sum of the TA recovered from the loading process.

3.2. Conductivity measurements

Phase inversion was monitored by measuring the conductivity of the emulsion external phase as a function of temperature using a conductivity meter (Jenway 4330, UK). Measurements were made at 1 °C intervals, starting at 55 °C. The phase inversion process and conductivity measurements were repeated at three concentrations of NaCl (2%, 3%, and 5%, w/w) to assess the effect of ionic strength upon the particle production process.

3.3. High performance liquid chromatography

The HPLC analysis of TA was performed using a system consisting of a 200 LC pump, a 200 LC autosampler and a 284 UV detector (Perkin-Elmer, UK). Separation was achieved using a Kromasil C18, (250 mm × 4.6 mm, pore size: 100 A, surface area: 340 m^2/g, carbon load 19.0%) column at room temperature. The mobile phase consisted of a degassed and filtered 50:50 mixture of ethanol/methanol which was pumped through the column at a rate of 1 ml/min. The sample injection volume was 50 μl and TA was detected at 284 nm over a 15 min run time. The TA peak eluted at 8.30 ± 0.11 min (n = 108) and the solvent front at approximately 4 min.

3.4. Particle size analysis

The mean effective volume diameters (M_{EVD}) and the polydispersity index of nanoparticles were determined by photon correlation spectroscopy (PCS) using a Zetasizer 90plus (Brookhaven, USA) fitted with a 488 nm fixed angle (90°) laser beam at 25 °C. A mean polydispersity index and size was calculated by the average of three nanoparticle batches. All batches were diluted with deionised filtered water (0.45 μm Nalgene filter, BDH, UK) to produce dilutions of up to 1:200 prior to measurement (also performed in a triplicate). The actual size of the nanoparticles were estimated by extrapolating a graph of size vs. particle concentration to determine the M_{EVD}.

3.5. Physical stability

The fabricated placebo nanoparticles (P_{LN}) and the TA loaded nanoparticle both pre (TA_{LN}) and post purification ($TA_{LN\text{-}PURE}$) were divided into different batches, protected from light and stored at three different temperature conditions (4 °C, 25 °C, and 40 °C). Particles size measurements were performed using PCS after 7, 14, and 28 days of storage for each sample, at each temperature.

3.6. Formulation preparation and rheological measurement

The gel was prepared by adding HA powder (2%, and 1.5 w/w) to the purified TA nanoparticles (80%, w/w) and allowing the system to hydrate for 24 h at 24 °C. The rheological testing was performed using CSL a cone and plate rheometer (Carri-med, USA) with plate diameter of 4.0 cm and cone angle of 1.510° at a 100 μm fixed gap. The test was performed over a 1–10 Hz frequency range (shown not to irreversibly damage the gel structure, data not shown) at constant stress amplitude of 0.789 Pa. All the measurements were carried out at 20 °C. Twenty data points were recorded for each rheogram; three replicates were performed for each formulation.

3.7. Nanoparticle tracking analysis (NANOSIGHT LM10™)

A 250 μl sample containing the particles at a theoretical concentration in the range $1 \times 10^{7-9}$/mL was introduced into a scattering cell through which a focused laser beam (40 mW at either 404 or 635 nm) was passed. Particles within the path of the laser beam were observed via a microscope-based system (Brunel Microscopes UK) onto which was fitted a CCD camera (Marlin CCD, Allied Vision Technologies). The motion of the particles in the field of view (approx. 100×100 μm) was recorded at 30 frames per second and the subsequent video analysed using the NanoSight Nanoparticle Tracking Analysis Software 'NTA 2.0. Build 0122' (NanoSight, UK). Each particle visible in the image was individually, but simultaneously tracked from frame to frame and the mean square displacement particle, diffusion coefficient and particle size was calculated using the NanoSight software (NanoSight, UK). The diffusion coefficient (Dt) and hence sphere equivalent, hydrodynamic radius (rh) was determined using the Stokes–Einstein equation (Eq. (3)):

$$Dt = \frac{KBT}{6\pi\eta rh} \quad (3)$$

where KB is Boltzmann's constant, T is temperature and η is viscosity.

3.8. In vitro permeation studies

Permeation studies were conducted using pre-calibrated, upright Franz diffusion cells with an average surface area of 0.5 cm^2 and an average receiver compartment volume of 2.5 mL (MedPharm Ltd, Surrey UK). The pig skin membrane was prepared by removing the subcutaneous fat from the pig cheek using forceps and a scalpel. Individual sections of fat-free skin (of adequate size to fit in the Franz diffusion cells) were cut using a cork borer and washed using distilled water. Full thickness pig skin was sealed between the donor and receiver chamber of the Franz diffusion cells using parafilm and the cells were partially submerged in a water bath on a magnetic stirrer plate (Varimag, Telesystem HP15, Daytona, FL, USA) at 37 °C. Triglyceride oil Miglyol 810 (SBlack, UK) was selected as a receiver fluid (in vitro method previously described in Moddaresi et al., 2010). The cells were allowed to equilibrate in the water bath for 1 h prior to experiment initiation. They were inverted for 1 min to check for leakage, after which an equivalent finite dose (377.7 μg/cm^2) was applied on the apical surface of the skin using a pre-calibrated positive displacement pipette (Gilson, US). After 24 h, a 0.5 mL sample was taken from the receiver fluid and a mass balance recovery from the SC, epidermis and dermis was performed. The Franz cells were dismantled and both receiver and donor compartments washed with ethanol. The washings were collected, made up to a known volume and assayed by HPLC. The skin was cleaned with cotton buds and mounted on a firm base. Tape stripping was performed using Ultra clear Scotch tape (Sellotape, UK). Each piece of tape was placed on the whole area, a defined pressure was applied (using 300 mg weight) for 10 s and the tape was peeled from the test site with forceps. The first 2 strips were considered as containing residual formulation and were added to the cotton buds, soaked in ethanol for 24 h, the solution filtered and assayed by HPLC. The 22 subsequent strips removed from the skin were collected and defined as containing the TA that had permeated into the SC. TA was extracted from the tapes by adding ethanol, shaking for 6 h, filtering and assaying by HPLC. The TA–skin extraction method was shown to have a recovery of 104.9% ± 12.4%.

3.9. Statistical analysis

All data were presented as a mean ± standard deviation (SD). After conducting normality test, a parametric one-way ANOVA test was used for normally distributed data and a nonparametric ANOVA for non-Gaussian distributed data. For all pair-wise comparisons of means, t-test was applied. The significance level was 0.05 throughout.

4. Results

4.1. Nanoparticle production

The phase inversion process of the emulsions was monitored by measuring the conductivity of the emulsion's external phase as a function of temperature. At the start of the heating cycles, i.e. at 55 °C, the emulsions displayed high conductivity values (3000 μS/cm for 2% NaCl, 4000 μS/cm for 3% NaCl, 5000 μS/cm for 5%), which was indicative of the mixture components forming an o/w emulsion. Increasing the temperature of the emulsion resulted in a rapid decrease in conductivity. For example, in the last temperature cycle at ca. 90 °C all the conductivity measurements were lower than ca. 100 μS/cm irrespective of NaCl concentration (Fig. 1). The phase inversion temperature (PIT), defined as the midpoint of the exponential region of the temperature vs. conductance graph for an emulsion in the last cycle of the manufacturing process (Walde et al., 1997), was 84.5 °C, 86.5 °C, and 87.0 °C when using 5%, 3%, and 2% NaCl, respectively.

4.2. Nanoparticle characterisation

The P_{LN} displayed a M_{EVD} ($n = 3$) of 53.2 ± 2.0 nm with a polydispersity of 0.05 ± 0.01 prior to purification, and 50.8 ± 0.5 nm with a polydispersity of 0.02 ± 0.01 after the purification process (data not shown graphically). TA_{LN} displayed a size of 55.1 ± 1.0 nm (polydispersity of 0.08 ± 0.02), and 54.0 ± 1.40 nm (polydispersity of 0.05 ± 0.01), before and after purification, respectively ($n = 3$). A lack of significant difference (t-test, $p > 0.05$) in LN size before and after purification for both the P_{LN} and the TA_{LN} batches indicated that the nanoparticles remained intact during the centrifugation process. In addition, the significant reduction (t-test, $p < 0.05$) in particle size polydispersity for both the placebo and TA loaded nanoparticles after purification indicated that the excess manufacturing excipients were successfully being isolated from the LN. Determining the TA content of the LN after loading using the HPLC method showed that the TA loading process was both efficient and reproducible (57.7 ± 4.9% loading efficiency).

4.3. Physical stability

Upon storage, the mean M_{EVD} of the P_{LN} at 4 °C, 25 °C, and 40 °C did not increase significantly (one-way ANOVA, $p < 0.05$). This was also found to be the case after loading TA into the LN, and storing the particles at 25 °C and 40 °C for 28 days. However, at 4 °C, the M_{EVD} of the TA_{LN} significantly increased by 5.0% ± 0.01. After purification the LN were more susceptible to size changes. The purified TA_{LN} increased significantly in size ($p > 0.05$, t-test) by 11.9% ± 0.01, 10.1% ± 0.02, and 9.0% ± 0.01 at 4 °C, 25 °C, and 40 °C, respectively during 28 days of storage (Table 1).

4.4. Nanoparticle–vehicle interactions

The change in rheological properties of the semi-solid formulations in response to nanoparticle addition was measured using a constant strain in the linear viscoelastic regions for the materials (previously determined, data not shown). The storage (elastic)

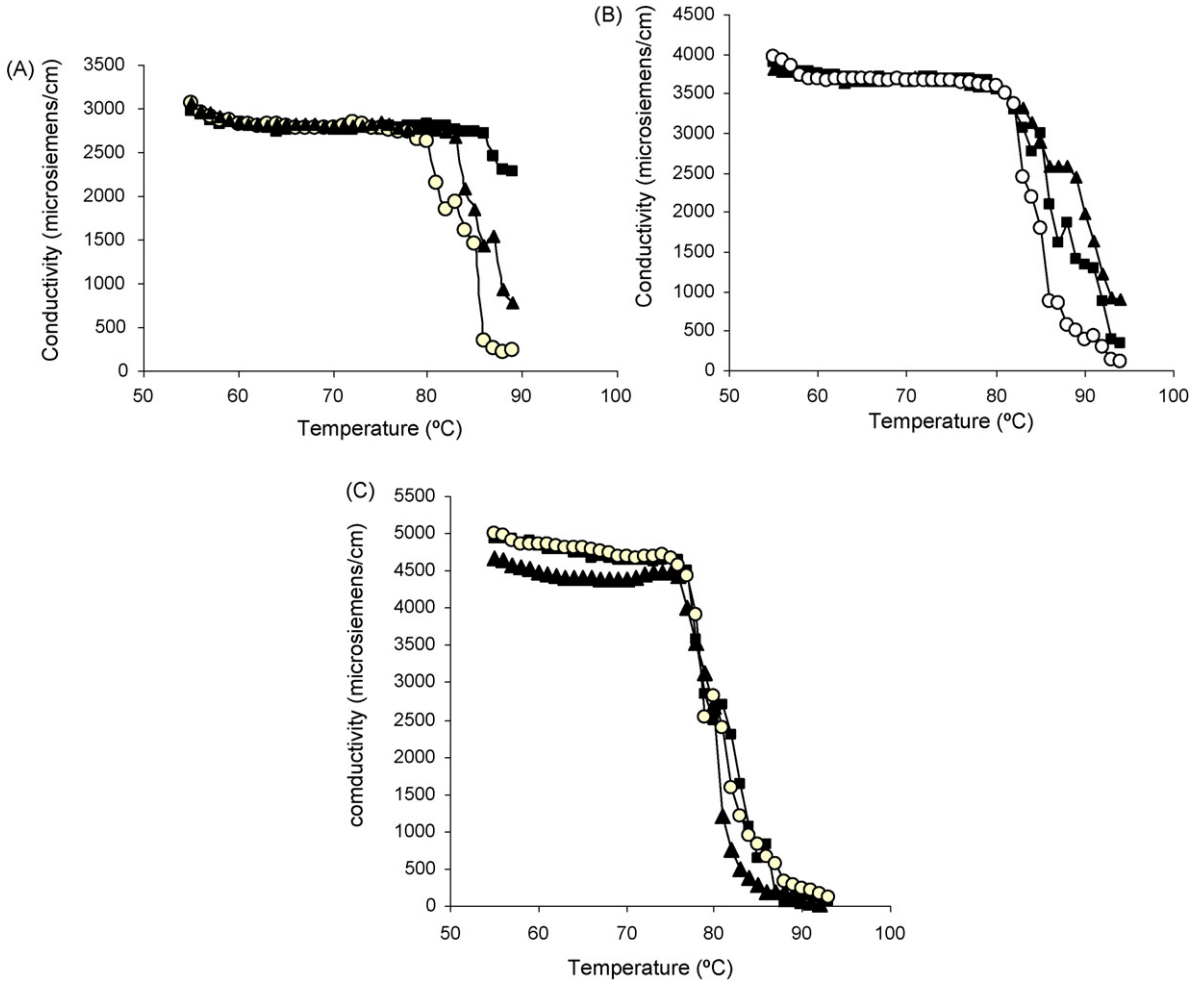

Fig. 1. Conductivity measurements obtained during lipid nanoparticle production, with different concentrations of sodium chloride in the aqeouse phase. (A) 2% NaCl, (B) 3% NaCl, (C) 5% NaCl. Closed square represents heating cycle 1, closed triangle represents heating cycle 2 and open circle represents heating cycle 3. Each data point represents a single reading.

modulus (G') and loss (viscous) modulus (G'') were measured for two HA gels containing 1.5 and 2% (w/w) HA, with and without the addition of the TA loaded LN (TA_{LN} and $TA_{LN\text{-}PURE}$). The addition of the LN to the HA gels affected their rheological behaviour, measured as a function of frequency (Fig. 2). The 2% HA gel displayed a higher storage modulus (G') at low stress frequencies, compared to the loss modulus (G''), however the addition of the purified LN dispersion to the gel inverted the storage vs. loss modulus trend (Fig. 2A). An incremental increase in the concentration of LN dispersion resulted in incrementally reduced cross over frequency (Fig. 3). For example, adding 80% TA-LN to 1.5% and 2% HA gels significantly ($p < 0.05$) decreased the crossover frequency in both cases (7.3 ± 0.4 to 4.8 ± 0.2 Hz and from 2.96 ± 0.2 to 1.97 ± 0.5, respectively, $n = 3$, Fig. 3). A lower crossover frequency indicates a greater system stability, and an increase in viscoelasticity hence these results suggest the presence of a strong HA–nanoparticle interaction. Altering the concentration of HA in the gel dramatically altered the viscoelastic properties of the gel. Increasing the percentage of HA in the gel from 1.5% to 2% approximately doubled the G' and G'' values and halved the cross over frequency indices.

The absolute size of the nanoparticles, when measured by the NTA system, was slightly larger than the PCS size at ca. 100 nm. Although the particle size did vary significantly ($p = 0.036$, ANOVA), when the particle concentration was altered these changes had no pattern and thus it was assumed to be a consequence of the sample-sample error. In general, the nanoparticle diffusion coefficient increased as the HA gel samples were diluted, that is, the particle and HA concentration was reduced. At similar particle concentrations (5×10^{-8} particles per mL) the diffusion coefficients for the LN in the HA matrix were lower at 324.0 ± 23.0 (cm^2/s) than when the LN were suspended in water 478.0 ± 80.0 (cm^2/s) (t-test, $p < 0.05$; $n = 3$, Table 2).

Table 1
Average effective lipid nanoparticle diameter of placebo lipid nanoparticles (P_{LN}), TA-loaded nanoparticles (TA_{LN}) and purified TA-loaded nanoparticles ($TA_{LN\text{-}PURE}$) at different storage temperatures. Data represent the mean ± standard deviation of 3 independent batches of nanoparticles.

		Average effective diameters (nm)		
		4 °C	25 °C	40 °C
1 day	P_{LN}	58.0 ± 1.5	58.4 ± 1.5	58.9 ± 0.4
	TA_{LN}	55.6 ± 0.5	55.8 ± 0.4	56.6 ± 0.7
	$TA_{LN\text{-}PURE}$	54.4 ± 0.4	54.5 ± 0.4	55.1 ± 1.2
7 days	P_{LN}	58.6 ± 1.6	61.2 ± 0.3	61.0 ± 0.4
	TA_{LN}	56.5 ± 0.7	56.8 ± 0.8	57.5 ± 0.6
	$TA_{LN\text{-}PURE}$	55.6 ± 1.3	55.3 ± 0.3	58.5 ± 0.4
14 days	P_{LN}	60.5 ± 0.6	60.8 ± 0.1	60.7 ± 2.1
	TA_{LN}	58.5 ± 1.0	57.5 ± 0.5	57.7 ± 0.6
	$TA_{LN\text{-}PURE}$	56.5 ± 0.8	58.9 ± 1.0	60.7 ± 2.2
21 days	P_{LN}	61.3 ± 0.4	61.5 ± 0.1	60.7 ± 2.2
	TA_{LN}	58.6 ± 0.7	58.6 ± 0.7	59.8 ± 1.2
	$TA_{LN\text{-}PURE}$	61.7 ± 0.7	60.6 ± 0.8	60.5 ± 0.6

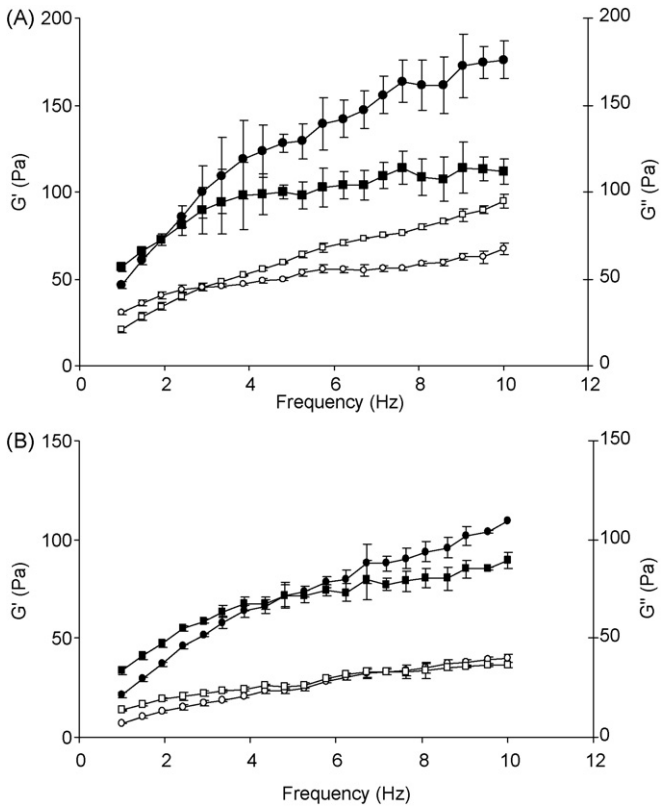

Fig. 2. Storage modulus (circle – G') and loss modulus (square – G'') measured as a function of frequency (Hz) at 20 °C for hyaluronic acid (HA) gels (open symbols) and HA gels prepared with a TA-loaded purified lipid nanoparticle suspension (TA_{LN} – closed symbols). (A) 2% HA, 18% water and 80% purified TA_{LN}; (B) 1.5% HA gel with 18.5% water and 80% purified TA_{LN}. Data points represent mean ± standard deviation, $n = 3$.

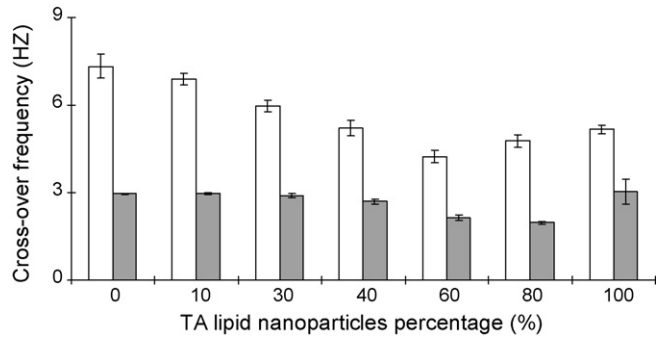

Fig. 3. Cross over frequencies, i.e. points where elasticity modulus (G') is equal to viscosity modulus (G''), for two hyaluronic acid (HA) gels containing tocopheryl acetate loaded lipid nanoparticles. 1.5% (w/w) HA (white bars), 2% (w/w) HA (grey bars). Data points represent mean ± standard deviation, $n = 3$.

Table 2
Average size and diffusion coefficient of purified TA-loaded nanoparticles ($TA_{LN\text{-}PURE}$) at different particle concentrations, with and without hyaluronic acid (HA). Data represent mean ± standard deviation of 3 independent nanoparticle samples.

Sample	Concentration (1×10^8 per mL)	Size (nm)	Diffusion coefficient (1×10^{-9} cm^2/s)
$TA_{LN\text{-}PURE}$	7.5 ± 0.8	101.3 ± 2.5	384.0 ± 20.2
	3.8 ± 0.5	90.7 ± 5.5	420.3 ± 62.2
	4.9 ± 4.0	120.3 ± 21.2	478.0 ± 80.0
HA + $TA_{LN\text{-}PURE}$	5.2 ± 0.4	117.7 ± 9.3	324.0 ± 28.2
	2.5 ± 0.3	128.0 ± 9.8	360.0 ± 43.3
	2.0 ± 2.2	91.3 ± 5.7	494.3 ± 25.0

Table 3
Skin deposition of tochopheryl acetate (TA) from hyaluronic acid gels (1.5% vs. 2%) with 80% (w/w) purified tochopheryl acetate loaded nanoparticles (TA-LN). TA was recovered after 24 h of administration (mean ± standard deviation, $n = 6$).

Compartment (μg/cm^2)	Formulation	
	$TA_{LN\text{-}PURE}$ 2% HA	$TA_{LN\text{-}PURE}$ 1.5% HA
Applied dose	377.65 ± 29.6	372.0 ± 13.7
Donor compartment	29.50 ± 19.8	54.8 ± 15.5
Skin surface	263.90 ± 42.1	289.7 ± 25.2
SC, tape strips	3.15 ± 2.3	4.3 ± 4.0
Viable epidermis	6.51 ± 2.6	6.1 ± 1.6
Receptor fluid	0	0
Total recovery, %	79.5 ± 9.3	95.5 ± 5.9

4.5. Permeation studies

Using a tape-stripping technique on pig skin to assess the delivery of TA from $TA_{LN\text{-}PURE}$ (80%, w/w) when loaded in both 1.5% and 2% HA gels demonstrated that 1.15 ± 1.07%, and 0.84 ± 0.65% of the applied dose, respectively was deposited in the SC (no significant difference, t-test, $p = 0.56$). In addition, 1.65 ± 0.47% and 1.73 ± 0.77% of applied TA dose was found in the epidermis/dermis when delivering the active using 1.5% and 2% HA gels, respectively (no significant difference, t-test, $p = 0.83$). The total TA recovery (mass balance) was 95.83 ± 5.86% and 79.52 ± 9.26%, for 2% and 1.5% HA gel, respectively, with standard deviations of below 4% ($n = 6$) for each compartment (Table 3).

5. Discussion

Nanoparticle production is often problematic as it is difficult to generate particles with a size of <100 nm that efficiently incorporate an active molecule, whilst retaining their physical stability during manufacture, storage and use. The phase inversion method, previously described by Heurtault et al. (2002), is a very robust means to fabricate nanoparticles. It generates nanosized particles from a highly stable nanoemulsion in a 'one pot' reaction. The specific nanoemulsion employed in this work was composed of medium chain triglycerides, phospholipids and the surfactant Solutol®. The hydrophilic/lipophilic balance (HLB) of Solutol®, a non-ionic ethoxylated surfactant, is known to be temperature dependant; it becomes less hydrophilic upon heating (Miller et al., 2001). The change in HLB of Solutol when heated promotes the conversion of w/o emulsion to o/w emulsion during temperature cycling and this can be used to homogenise the emulsion. It has previously been suggested that addition of NaCl to the aqueous phase dehydrates the polyoxyethylene chain of the Solutol and consequently affects its solvency and the PIT point (Selker and Sleicher, 1965; Enever, 1976). However, in the current study, the monitoring of the phase inversion process using conductivity demonstrated that the addition of increasing concentrations of electrolytes to the aqueous phase of the emulsion had a minor effect on PIT point (Fig. 1). For example, increasing the NaCl levels from 2% to 5% shifted the phase inversion temperature from 87.0 °C to 84.5 °C.

The solid shell of the LN, which has previously been reported to form around the particles generated from this process (Heurtault et al., 2002), facilitated the separation of the LN from the excess drug and excipients in the mixture. Particle aggregation which is usually driven by van der Waals attraction was presumably prevented in the non purified suspensions by the non-ionic surfactant that was proposed to adsorb to the surface of the solid shell (Cevc and Richardsen, 1999). The negative effect of the purification process on the physical stability could have been a result of the impurities in the surfactant that were lost during purification or due to the removal of large amounts of the surfactant molecules during centrifugation. Regardless of the cause the aggregation was minimal

and not considered to have a significant effect on results from this work (Westesen and Siekmann, 1997).

It is important to note that, in the context of particle size measurement, the limitations of the photon correlation spectroscopy (PCS) technique may have influenced the data derived in this study. PCS produces inaccurate results if the sample is too concentrated, due to back scattering effects, therefore the nanosuspensions require significant dilution prior to measurement. Nanosuspension dilution can cause changes in the particle size as a result of swelling or desorption of surfactants from the nanoparticle surface, if the system shows poor stability (Muller, 1990). However, by deriving the size of the particulates from the intercept of the size vs. concentration graphs the concentration/stability effects were minimised.

The rheological properties of semi-solid vehicles are important as they have the potential to affect the sensory feeling of formulations and the contact of any incorporated active with the surface of the skin (Rafiee-Tehrani and Mehramizi, 2000). Furthermore, in a delivery system where a nanocarrier is employed to administer an active, the viscoelastic properties of a topical formulation could also have a pronounced influence on the movement of the nanocarrier. The mobility of the nanoparticles in the formulation will be dependent upon the nanoparticle–vehicle interactions, if any are present. It is important when considering the resistance of a semi-solid material to flow to understand where the resistance originates, so that the measurements can be interpreted in the correct context.

HA, a naturally occurring polysaccharide, has been shown to form a gel-like system without any additives (Cowman et al., 1998). It forms strong intra and inter-molecular interactions even at low concentrations. Previously, it was reported that inclusion of small molecules such as phospholipids disturb the inter-molecular interaction in HA gel network, reduce the entanglement between the molecules and decrease both the viscous and elastic moduli (Ghosh et al., 1994; Kobayashi et al., 1994; Pasquali Ronchetti et al., 1997; Mo et al., 1999). Adding LN to the gels in this study not only increased both the elastic (G') and viscous (G'') moduli of the HA gel network over the measured frequency range, but also decreased the crossover frequencies. An increase in macroviscosity of the HA gels in response to LN addition was indicative of the LN interacting with the HA chains. Nanoparticles improving the extent or strength of the crosslinking within the gel is a phenomenon that has been reported previously (Lippacher et al., 2001; Souto et al., 2004). In addition, it has been previously demonstrated that the strengthening of the HA network can be related to immobilisation of water in the HA gel (Kobayashi et al., 1994). Adding NP to HA gel certainly enhances the amount of amphiphilic surfaces upon which water can bind (due to small size of TA-LN, <60 nm) and as such a similar water immobilisation hypothesis may be the reason for the strengthening of the gel structure herein.

Given the innate ability of HA to form extensive cross links, it was not surprising that the particle diffusion coefficients generated in this work were dependent on the HA concentration. Increasing the concentration of HA in aqueous solutions is known to alter solution microviscosity and to lead to decrease in particle mobility (Scott et al., 1991; Balzer et al., 1995). The nanoparticle gels required dilution beyond the range normally employed to form a semi-solid preparation to facilitate NTA to be performed, however HA is known to be a polymer that modifies both micro and macroviscosity at extremely dilute concentrations (Scott, 1989). The purpose of NTA in this study was to asses if the addition of HA to the LN suspensions altered particle mobility and if this was dependant on HA concentration. The absolute concentration of the HA gel present during the NTA therefore was not considered to be critical. Combining the results from the traditional cone and plate rheological measurements and the NTA led to the conclusion that increasing either the LN concentration or the HA concentration in the gel led to the reduction in LN mobility (Balzer et al., 1995). Varying the HA concentration when the LN concentration was high was selected as the most appropriate test system to evaluate the influence of NP mobility upon drug delivery, as this presented significant drug to the surface of the skin whilst modifying the particle mobility in the gels.

There was no statistical difference in the amount of TA recovered from the strips and viable epidermis/dermis, regardless of type of HA formulation applied to the pig skin. Traditional theory suggests that for compounds with low aqueous solubility an increase in a formulation's viscosity (adding gelling polymers) leads to decrease in drug release rate and hence a corresponding drop in skin permeation (Welin-Berger et al., 2001). However, this is only the case if release rate maintains an adequate concentration of drug in the solution state to allow diffusion through the semi-solid vehicle to be rate limiting (Petit et al., 1996). As reducing the LN particle mobility in the HA gel did not effect TA lipid penetration, it must be concluded that the delivery of hydrophobic therapeutic agents from NP suspended in semi-solid vehicles is dictated by drug release and not particle mobility.

6. Conclusions

The phase-inversion method used here was suitable for producing monodisperesed TA lipid nanoparticles of less than 100 nm in diameter. Adding purified TA nanoparticles to sodium hyaloranate led to a one step production system of a gel without any additives. Rheology measurements showed that LN interacted with the HA gel network and this reduced the LN mobility. However, reducing the mobility of the LN by increasing the HA gel viscosity did not affect the TA permeation. Drug release from lipid nanoparticles was the rate limiting step that hindered hydrophobic drug permeation into the skin and for such systems to deliver therapeutic agents to into or through this biological barrier an active strategy is required to enhance the availability of the agent at the vehicle–skin interface.

Acknowledgements

The authors would like to acknowledge the financial support from University of the Arts, London and thank Matthew Wright from Nanosight for performing the nanotracking measurements.

References

Balzer, D., Varwig, S., Weihrauch, M., 1995. Viscoelasticity of personal care products. Colloids Surf. A 99, 233–246.
Baroli, B., Ennas, M.G., Loffredo, F., Isola, M., Pinna, R., Lopez-Quintela, M.A., 2007. Penetration of metallic nanoparticles in human full-thickness skin. J. Invest. Dermatol. 127, 1701–1712.
Cevc, G., Richardsen, H., 1999. Lipid vesicles and membrane fusion. Adv. Drug Deliv. Rev. 38, 207–232.
Chi, S.C., Jun, H.W., 1991. Release rates of ketoprofen from poloxamer gels in a membrane less diffusion cell. J. Pharm. Sci. 80, 280–283.
Cowman, M.K., Liu, J., Hittner, D.M., Kim, J.S., 1998. In: Laurent, T.C. (Ed.), Hyaluronan Interactions: Salt, Water, Ions. London Portland Press, pp. 17–25.
Dingler, A., Hildebrand, G., Niehus, H., Muller, R.H., 1998. Cosmetic antiaging formulation based on vitamin E-loaded solid lipid nanoparticles. Proc. Int. Symp. Control. Release Bioact. Mater. 25, 433–434.
Dingler, A., Krohs, S., Lukowski, G., Gohla, S., Muller, R.H., 1996. SLN (solid lipid nanoparticles) as new solid carrier of active ingredients in cosmetics. Eur. J. Pharm. Sci. 4, 148–155.
Enever, R.P., 1976. Correlation of phase inversion temperature with kinetics of globule coalescence for emulsions stabilized by a polyoxyethylene alkyl ether. J. Pharm. Sci. 65, 517.
Ghosh, P., Hutadilok, N., Adam, N., Lentini, A., 1994. Interactions of hyaluronan (hyaluronic-acid) with phospholipids as determined by gel-permeation chromatography, multi-angle laser-light-scattering photometry and H-1-Nmr spectroscopy. Int. J. Biol. Macromol. 16, 237–244.
Heurtault, B., Saulnier, P., Pech, B., Proust, J.E., Benoit, J.P., 2002. A novel phase inversion-based process for the preparation of lipid nanocarriers. Pharm. Res. 19, 875.

Jenning, V., Hildebrand, G., Gysler, A., Muller, R.H., Schaefer-Korting, M., Gohla, S., 1999. Solid lipid nanoparticles (SLNTM) for topical application: occlusive properties. Proc. Int. Symp. Control. Release Bioact. Mater. 26, 406.

Jenning, V., Schaefer-Korting, M., Gohla, S., 2000a. Vitamin A-loaded solid lipid nanoparticles for topical use: drug release properties. J. Control. Release 66, 115–126.

Jenning, V., Thunemann, A.F., Gohla, S.H., 2000b. Characterisation of a novel solid lipid nanoparticle carrier system based on binary mixtures of liquid and solid lipids. Int. J. Pharm. 199, 167–177.

Kreuter, J., Mills, S.N., Davis, S.S., Wilson, C.G., 1983. Polybutylcyanoacrylate nanoparticles for the delivery of [75Se] norcholestenol. Int. J. Pharm. 16, 105–113.

Kobayashi, Y., Okamoto, A., Nishinari, K., 1994. Viscoelasticity of hyaluronic-acid with different molecular-weights. Biorheology 31, 235–244.

Lippacher, A., Mnller, R.H., Mader, K., 2001. Preparation of semisolid drug carriers for topical application based on solid lipid nanoparticles. Int. J. Pharm. 214, 9–12.

Miller, D.J., Henning, T., Grunbein, W., 2001. Phase inversion of w/o emulsions by adding hydrophilic surfactants: a technique for making cosmetics products. Colloids Surf. 185, 681–688.

Moddaresi, M., Brown, M.B., Turmbric, S., Jones, S.A., 2010. The influence of particle transport on the topical delivery of tochopheryl acetate-loaded solid lipid nanocarriers. J. Pharm. Pharmacol. 62, 762–769.

Mo, Y., Takaya, T., Nishinari, K., Kubota, K., Okamoto, A., 1999. Effects of sodium chloride, guanidine hydrochloride, and sucrose on the viscoelastic properties of sodium hyaluronate solutions. Biopolymers 50, 23–34.

Muller, R.H., Kreuter, J., 1999. Enhanced transport of nanoparticle associated drugs through natural and artificial membranes—a general phenomenon. Int. J. Pharm. 178, 23–32.

Muller, R.H., 1990. Colloidal Carriers for Controlled Drug Delivery and Targeting: Modification, Characterization and In Vivo Distribution. Wiss, Verl-Ges, Stuttgart, Germany.

Pasquali Ronchetti, I., Quaglino, D., Mori, G., Bacchelli, B., Ghosh, P., 1997. Hyaluronan-phospholipid interactions. J. Struct. Biol. 120, 1–10.

Petit, J.M., Roux, B., Zhu, X.X., 1996. A new physical model for the diffusion of solvents and solute probes in polymer solutions. Macromolecules 29, 6031–6036.

Rafiee-Tehrani, M., Mehramizi, A., 2000. In vitro release studies of piroxicam from oil-in-water creams and hydroalcoholic gel topical formulations. Drug Dev. Ind. Pharm. 26, 409–414.

Ricci, M., Puglia, C., Bonina, F., Di Giovanni, C., Giovagnoli, S., Rossi, C., 2005. Evaluation of indomethacin percutaneous absorption from nanostructured lipid carriers (NLC). J. Pharm. Sci. 94, 1149–1159.

Ryman-Rasmussen, J.P., Riviere, J.E., Monteiro-Riviere, N.A., 2006. Penetration of 746 intact skin by quantum dots with diverse physicochemical properties. Toxicol. Sci. 91, 159–165.

Santos Maia, C., Mehnert, W., Schafer-Korting, M., 2000. Solid lipid nanoparticles as drug carriers for topical glucocorticoids. Int. J. Pharm. 196, 165.

Sanders, N.N., De Smedt, S.C., Van Rompaey, E., Simoens, P., De Baets, F., Demeester, J., 2000. Cystic fibrosis sputum: a barrier to the transport of nanospheres. Am. J. Respir. Crit. Care Med. 162, 1905–1911.

Scott, J.E., 1989. In: Everend, D., Whelan, J. (Eds.), Secondary Structures in Hyaluronan Solution: Chemical and Biological Implications. John Wiley, Chichester, pp. 6–16.

Scott, J.E., Cummings, C., Brass, A., Chen, Y., 1991. Secondary and tertiary structures of hyaluronan in aqueous solution, investigation by rotary-electron microscopy and computer simulation. Biochem. J. 274, 699–705.

Selker, A.H., Sleicher, C.A., 1965. Factors affecting which phase will disperse when immiscible liquids are stirred together. Can. J. Chem. Eng. 9, 298–301.

Souto, E.B., Wissing, S.A., Barbosa, C.M., Muller, R.H., 2004. Evaluation of the physical stability of SLN and NLC before and after incorporation into hydrogel formulations. Eur. J. Pharm. Biopharm. 58, 83–90.

Scherer, D., 1992. Einfluß von Polybutylcyanoacrylat-Nanopartikeln auf die orale Absorption von Arzneistoffen. Dissertation, Frankfurt.

Spiedel, M., Jonas, A., Florin, E., 2003. Three-dimensional tracking of fluorescent nanoparticles with subnanometer precision by use of off-focus imaging. Opt. Lett. 28, 69–71.

Walde, A., Tesmann, H., Leonard, M., Forster, T., 1997. In: Rieger, M., Rhein, L. (Eds.), Phase Inversion in Emulsions: CAPICO Concept and Application. Marcel Dekker, pp. 207–223.

Welin-Berger, K., Neelissen, J.A.M., Bergenstahl, B., 2001. The effect of rheological behaviour of a topical anaesthetic formulation on the release and permeation rates of the active compound. Eur. J. Pharm. Sci. 13, 309–318.

Westesen, K., Siekmann, B., 1997. Investigation of the gel formation of phospholipid-stabilized solid lipid nanoparticles. Int. J. Pharm. 151, 35–45.